Electronic Supplementary Information.

Efficient Generation of Highly Crystalline Carbon Quantum Dots via Electrooxidation of Ethanol for Rapid Photodegradation of Organic Dyes.

Santiago D. Barrionuevo,[a] Federico Fioravanti,[b] Jorge M. Nuñez,[cdefg] Mauricio Llaver,[h] Myriam H. Aguirre,[fgi] Martin G. Bellino,[j] Gabriela I. Lacconi,[b] and Francisco J. Ibañez*.[a]

[a] *Instituto de Investigaciones Fisicoquímicas, Teóricas y Aplicadas (INIFTA). Universidad Nacional de La Plata - CONICET. Sucursal 4 Casilla de Correo 16 (1900) La Plata, Argentina.*

[b] *INFIQC-CONICET, Dpto. de Fisicoquímica, Facultad de Ciencias Químicas, Universidad Nacional de Córdoba, Ciudad Universitaria, (5000) Córdoba, Argentina.*

[c] *Resonancias Magnéticas-Centro Atómico Bariloche (CNEA, CONICET) S. C. Bariloche 8400, Río Negro, Argentina.*

[d] *Instituto de Nanociencia y Nanotecnología, CNEA, CONICET, S. C. Bariloche 8400, Río Negro, Argentina.*

[e] *Instituto Balseiro (UNCuyo, CNEA), Av. Bustillo 9500, S.C. de Bariloche 8400, Río Negro, Argentina.*

[f] *Instituto de Nanociencia y Materiales de Aragón, CSIC-Universidad de Zaragoza, C/ Pedro Cerbuna 12, 50009, Zaragoza, Spain.*

[g] *Laboratorio de Microscopías Avanzadas, Universidad de Zaragoza, Mariano Esquillor s/n, 50018, Zaragoza, Spain.*

[h] *Laboratorio de Química Analítica para Investigación y Desarrollo (QUIANID), Facultad de Ciencias Exactas y Naturales, Universidad Nacional de Cuyo / Instituto Interdisciplinario de Ciencias Básicas (ICB), CONICET UNCUYO, Padre J. Contreras 1300, (5500) Mendoza, Argentina.*

[i] *Dpto. de Física de la Materia Condensada, Universidad de Zaragoza, C/ Pedro Cerbuna 12, 50009, Zaragoza, Spain.*

[j] *Instituto de Nanociencia y Nanotecnología CNEA-CONICET, Av. Gral. Paz, 1499, San Martín, Buenos Aires, B1650, Argentina*

**Author to whom correspondence should be addressed: fjiban@inifta.unlp.edu.ar*

S1. Ethanol electro-oxidation in alkaline media with Ni Foams as WE

Here we briefly study the electro-oxidation of ethanol in alkaline media using a Nickel Foam as working electrode and a platinum wire as counter with respect an Ag/AgCl reference electrode. Electro-oxidation of ethanol in alkaline media with nickel electrodes has been developed by Fleischmann and collaborators[1,2], extremely important in the synthesis of carbon quantum dots from ethanol in alkaline media. According to Fleischmann et al the electro-oxidation of simple chain alcohol in such circumstances it's a 4 e^- mediated process, this process involves the formation of oxides in the working electrode as a reversible process and some radical intermediates.

---

1) $$OH^- + lower\ oxide \underset{fast\rightarrow}{\Leftrightarrow} higher\ oxide + H_2O + e^-$$

2) $$(organic\ substrate)_{sol} \underset{on\ higher\ oxide}{\Leftrightarrow} (organic\ substrate)_{ads}$$

3) $$Higher\ Oxide + (Organic\ Substrate)_{ads} \overset{*}{\Rightarrow} lower\ oxide + radical\ intermediate$$

$* rate\ determining\ hydrogen\ extraction$

4) $$Radical\ Intermediate + (n-1) higher\ oxide \underset{yields}{\Rightarrow} (n-1) lower\ oxide + product$$

This is a general route for the electro-oxidation of simple chain alcohols in alkaline media, with different metal catalyst. Recently, Barbosa et al[3] take this same approach and using an FTIR they determined the different participants involved in the electro-oxidation of ethanol on polycrystalline nickel in alkaline media; according to their findings we can establish:

Lower oxide	= Ni $(OH)_2$	= Nickel Oxide (II)
Higher Oxide	= NiO (OH)	= Nickel oxide hydroxide
Organic Substrate	= CH_3CH_2OH	= Ethanol
Radical Intermediate	= CH_3CHO	= Acetaldehyde
Product	= CH_3COOH	= Acetic Acid (Acetate for ph>10)

Yielding the next 5 equations for the electrode dynamics:

1) $$OH^- + Ni(OH)2 \underset{fast\rightarrow}{\Leftrightarrow} NiO(OH) + H_2O + e^-$$

2) $$(CH_3CH_2OH)_{sol} \underset{on\ higher\ oxide}{\Leftrightarrow} (CH_3CH_2OH)_{ads}$$

3) $$NiO(OH) + (CH_3CH_2OH)_{ads} \overset{*}{\Rightarrow} Ni(OH)2 + CH_3CHO$$

$* \; rate\ determining\ hydrogen\ extraction$

4) $$CH_3CHO + (n-1)NiO(OH) \underset{yields}{\Rightarrow} (n-1)Ni(OH)2 + CH_3COOH$$

5) $$CH_3COOH + OH^- \underset{yields}{\Rightarrow} CH_3COO^-$$

In order to study ethanol electro-oxidation, we perform several Cyclic Voltagrammetries in a 3-electrode set-up of a solution of 1M NaOH and 0.5 M EtOH. Figure S1A shows a schematic of the experimental set-up. Nickel Foam is used as a working electrode and a platinum wire as counter electrode. The reference voltage is set trough an Ag/AgCl reference electrode. Figure S1B shows a cyclovoltammetry measurement of ethanol electrooxidation on a Nickel foam. Control group without ethanol is added for completeness. Ethanol can be electrooxidized to Acetate in a 0.55-0.85 V window with respect to an Ag/AgCl reference electrode using Ni foam as a working electrode. The presence of Nickel Oxides is critical to the electro-oxidation of ethanol because these oxides are participants in all the intermediate reactions.

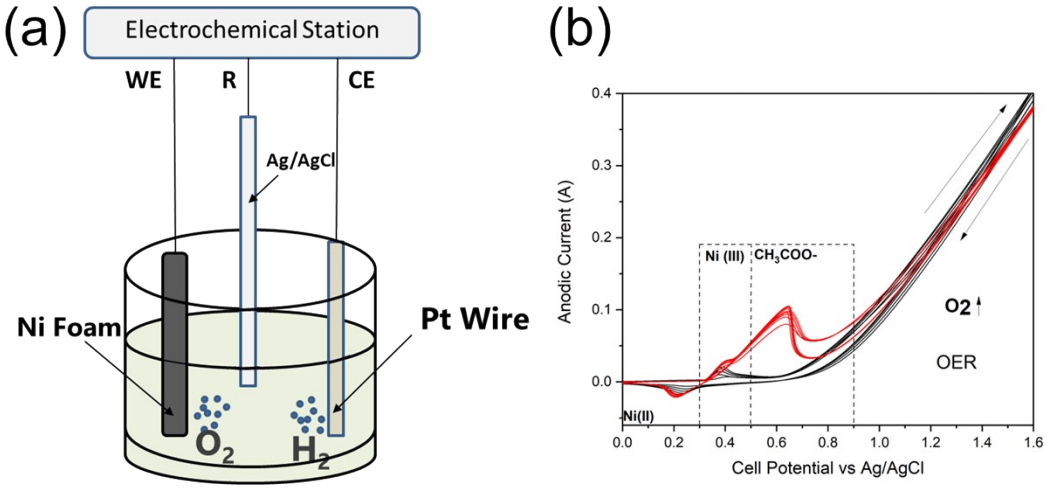

Figure S1. (a) Experimental set-up for study electrochemical oxidation of ethanol. (b) Ciclic Voltagramm of Nickel Foam in a NaOH 1M+ EtOH 0.5 M (in red) and Control Experiment (black) without EtOH.

S2 Insights into the Electrooxidation of Ethanol and CQDs formation. Section S1 and Figure S1 discusses the electrooxidation reaction of ethanol and exhibits cyclic voltagramm (CVs of the electrochemical reactions occurring at the anode). Carbon nanoparticles are produced in a bottom-up synthesis through dehydration and carbonization of ethanol during electrooxidation. These carbon nanostructures are generated at the interface of the working electrode in a media composed of a mixture of ethanol and 0.1 M NaOH which is subjected to 30 V for 1 h. One of the main products of electrooxidation of ethanol is acetaldehyde. When Ni is used as the working electrode, the preferred pathway of electrooxidation is a 4-electron mediated process where acetaldehyde and acetic acid are generated as intermediate and final product, respectively. [1,2] In the presence of Na and in a strong alkaline media, acetic acid deprotonates to form sodium acetate which precipitates upon saturation. Acetaldehyde is generated in large amounts upon ethanol electrooxidation and is the starting block in the bottom-up synthesis of CQDs through electrochemical oxidation of ethanol. During the synthesis, the concentration of acetaldehyde begins to build up at the interface of the working electrode as well as in the solution; eventually leading to an aldol addition and condensation process.[4] During aldol condensation, the conjugate base of an aldehyde adds to the carbonyl group of another aldehyde. This mechanism gives a new α, β-hydroxyl aldehyde which is dehydrated to form an α, β-unsaturated carbonyl compound. In the case of acetaldehyde, the aldol addition product is 3-hydroxybutanal, which could be dehydrated to yield crotonaldehyde. The aldol condensation of acetaldehyde is catalyzed by hydroxide ions (the main source in this case) via the formation of Ni $(OH)_2$ / NiO (OH) at the anode, offering basic sites for the process to occur and giving different self-regenerating phases of Ni $(OH)_2$ that push large amounts of acetaldehyde to enhance the process. This situation promotes the aldolization of crotonaldehyde with acetaldehyde resulting in the formation of hexa-2,4-dienal.[5] Repeating this process of aldol condensation produces higher molecular weight compounds that catalyzed, by the Ni, could give rise to a mechanism of cycloaddition. Also, different adsorbed species (for example $–CH_2CHO$) bonded to α, β unsaturated moieties could produce branched, long-chain molecules that are supported on the anode surface[6] and that we could see as sub product of the synthesis in the HRTEM characterization. Metal oxides are crucial to the production of acetaldehyde and the subsequent aldol condensation of the product, because there are less efficient catalysts when compared to Pt regarding the ethanol electrooxidation process. When Pt is used as a working electrode the preferred oxidation pathway leads to CO_2. This could be the reason why Liu et al[7] observed no CNs formation in their set up even though Deng et al[8] reported specifically on that manner.

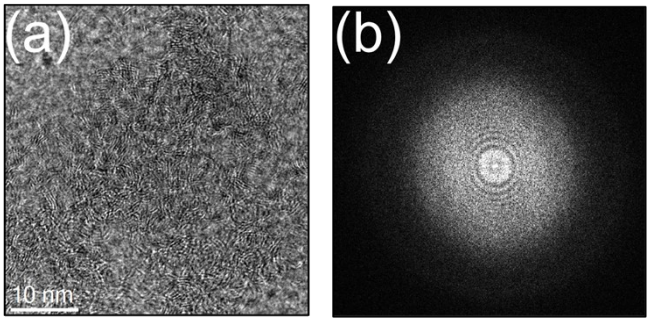

Figure S2. Branched, long-chain molecules as subproduct during electrooxidation of ethanol (a) and their corresponding FFT (b) showing amorphous phases.

S3. HRTEM image of CQD with several crystallographic directions.

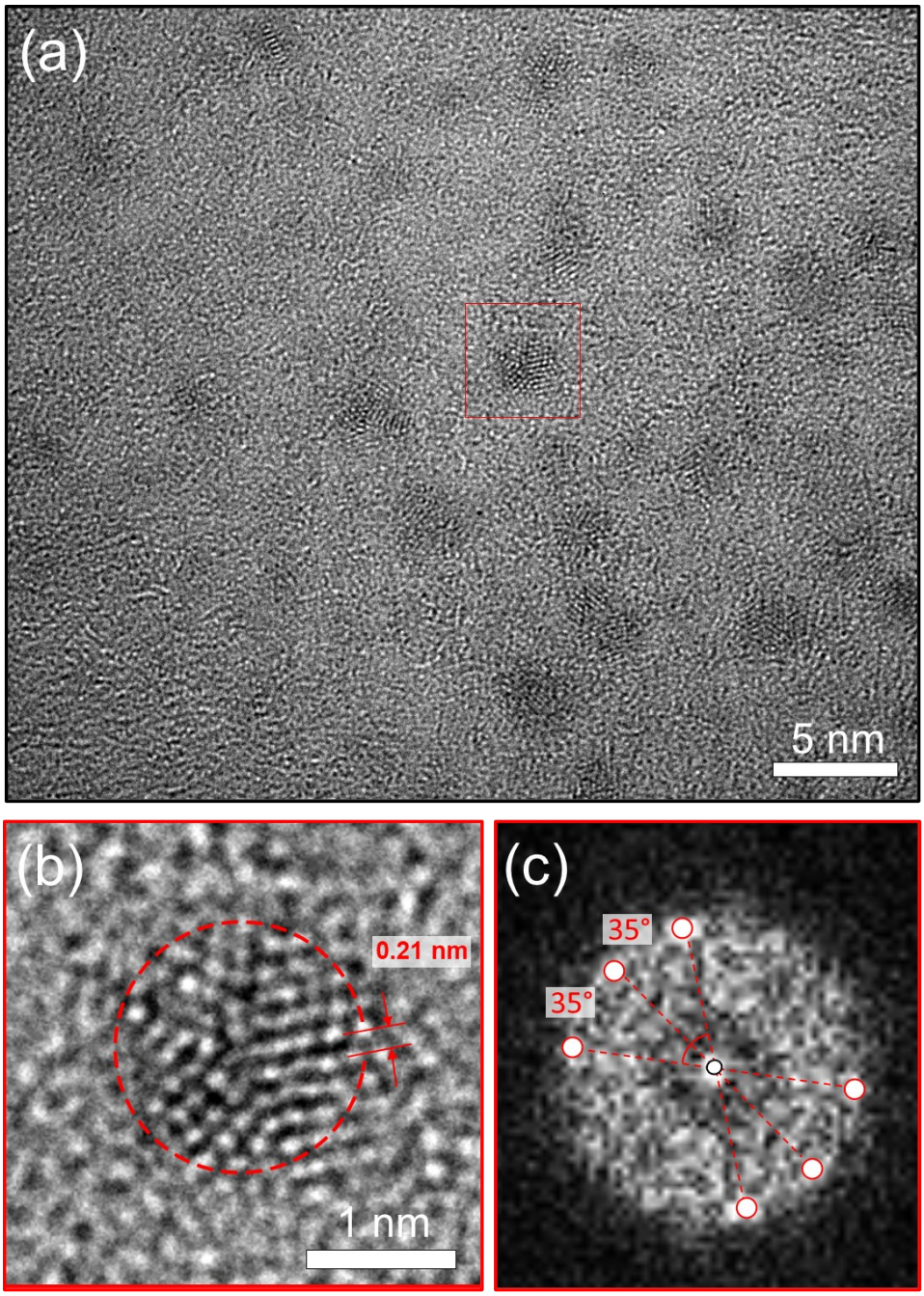

Figure S3. HRTEM image of another region of the sample (a). Digital zoom into the ROI showing different crystallographic directions (b). FFT of ROI.

S4. Lattice fringe of CQDs and Nanodiamonds

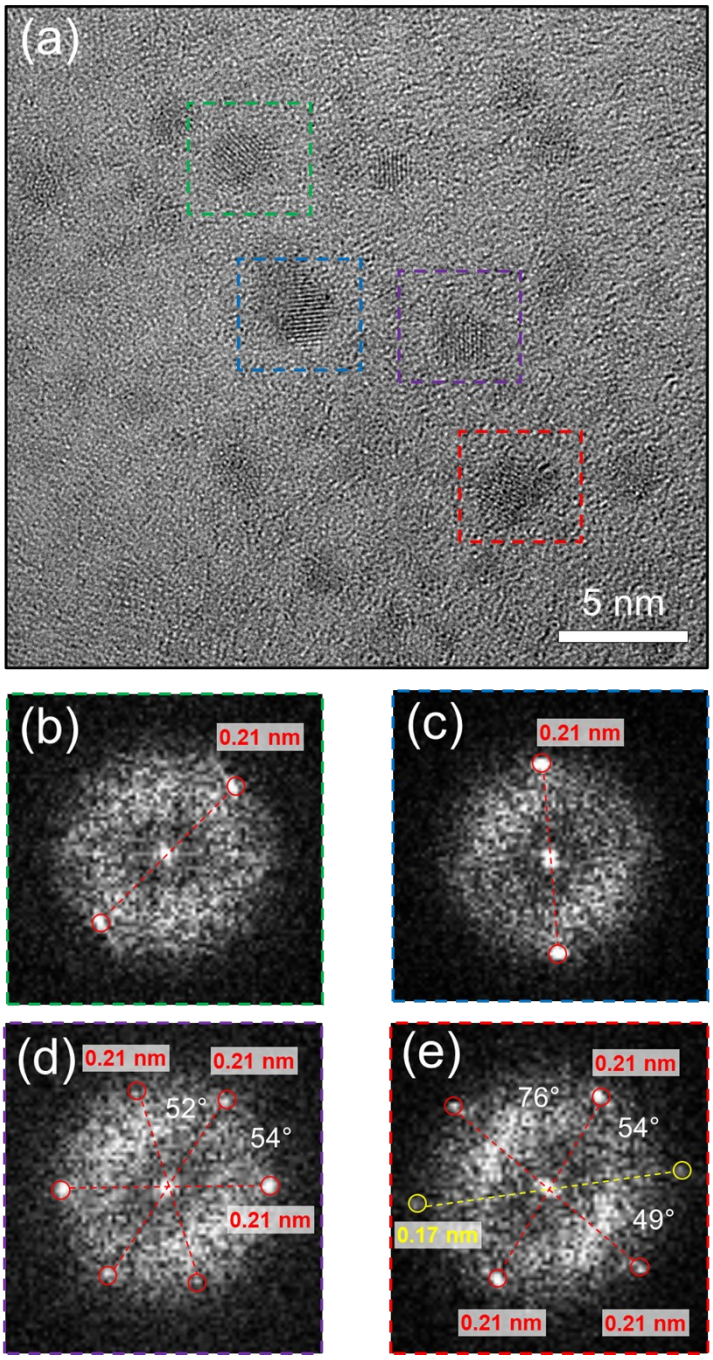

Figure S4. HRTEM image (a) in another zone of the aforementioned sample, different ROIs color coding is stablished in order to assess the crystallinity of different carbon nanoparticles. FFT of four ROI are color coded in green(b), blue (c), violet (d) and red (e).

S5. Comparative simulated UV-Vis spectra and emission properties of pyrene and pyrene + 2OH

# Rings sp^2 Domain	PAH	Emission Wavelength (nm)	Emission Energy (eV)	Transition
4	Pyrene	336.5	3.684	H-1 ↔ L (0.432897) H ↔ L+1 (0.562973)
4	Pyrene + 2 OH	365.6	3.391	H-1 ↔ L (0.78822) H ↔ L (0.033505) H ↔ L+2 (0.150889)

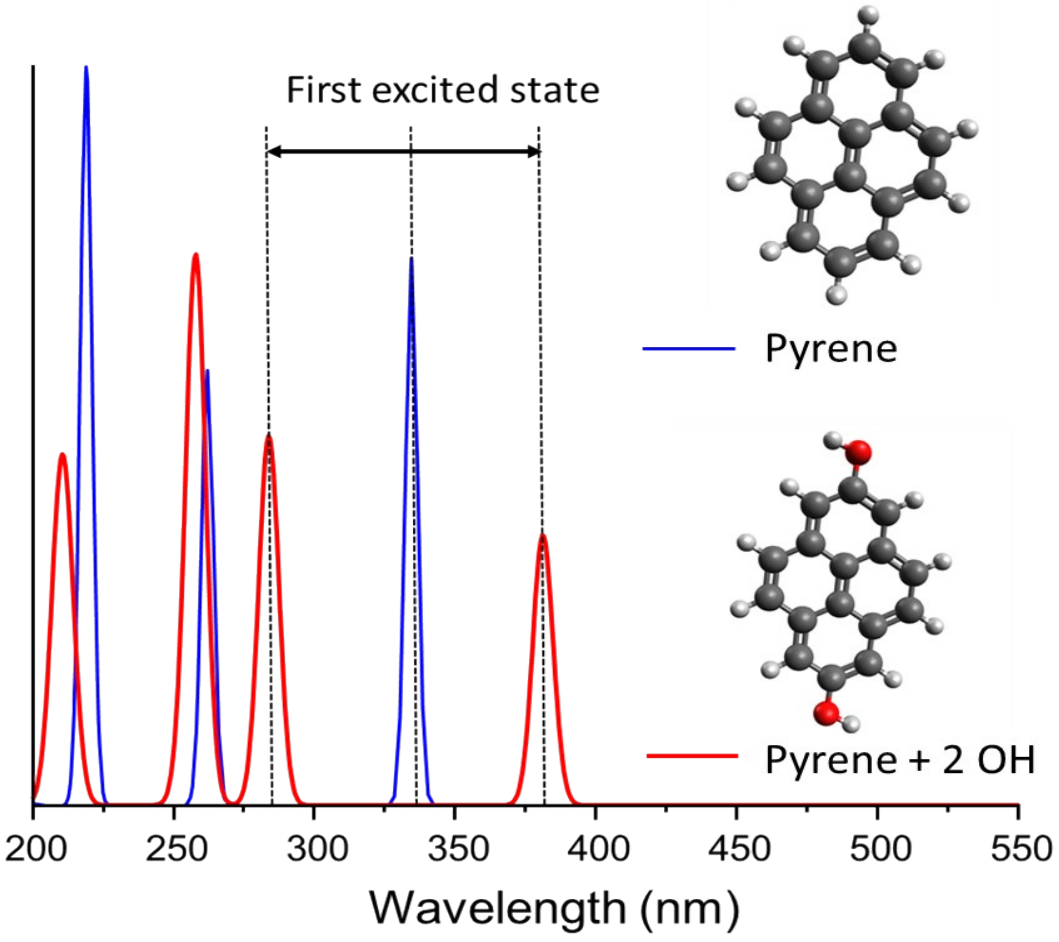

Figure S5. Simulated Uv-Vis Spectra and emission properties for Pyrene and Pyrene + 2OH

S6. Simulated Molecular orbitals for Coronene + charged carbonyl and orbital character classification.

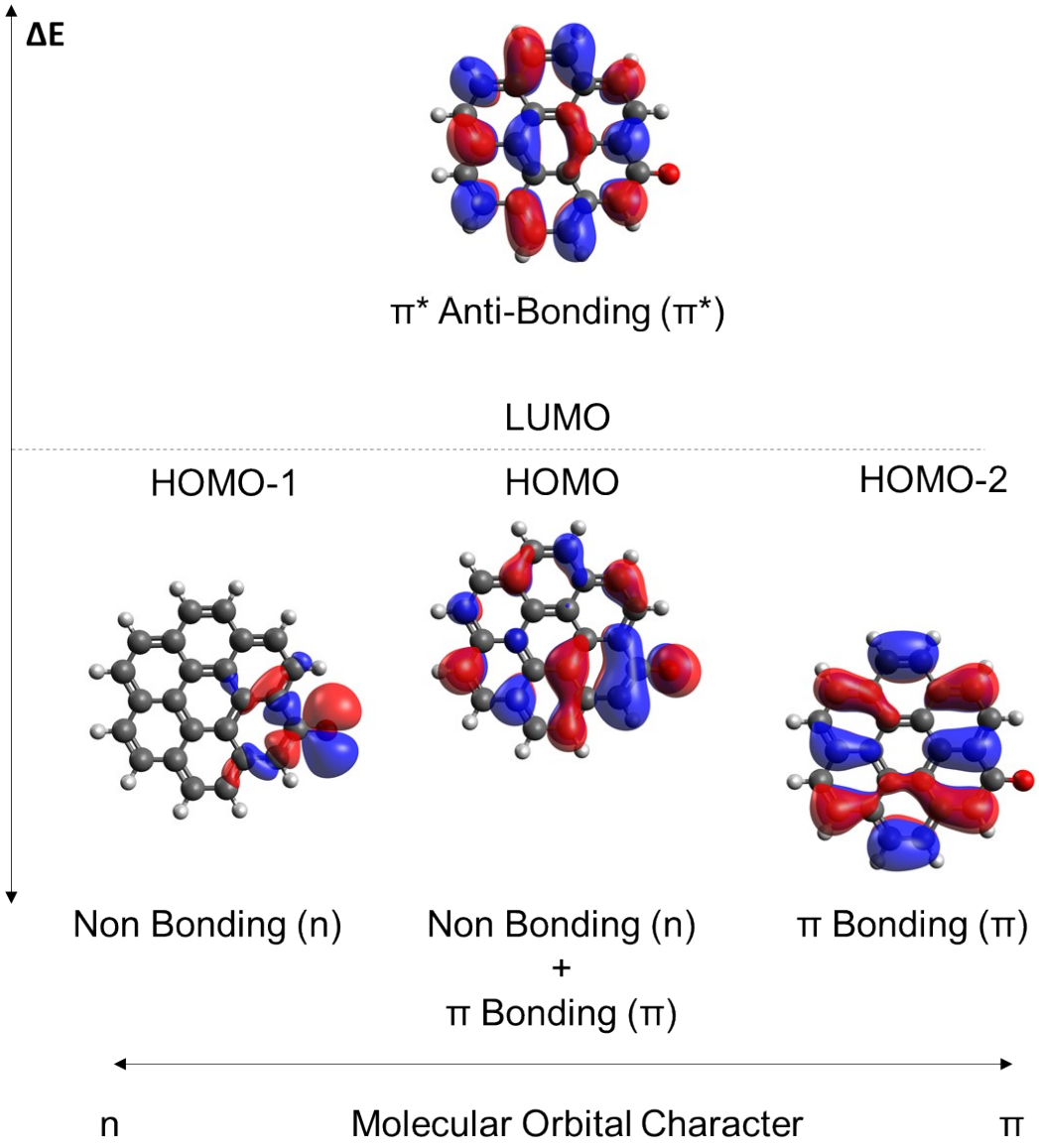

Figure S6. Simulated molecular orbitals for coronene+ charged carbonyl.

S7. Survey XPS spectra (0-600 eV) and C/O content for CQDs

Name	Peak (eV)	FHWM (eV)	Area (CPS * eV)	Atomic %
C1s	286.06	3.06	152991.76	76.77
O1s	532.6	3.74	78740.38	16.35
Na1s	1072.33	3.04	66694.39	6.88

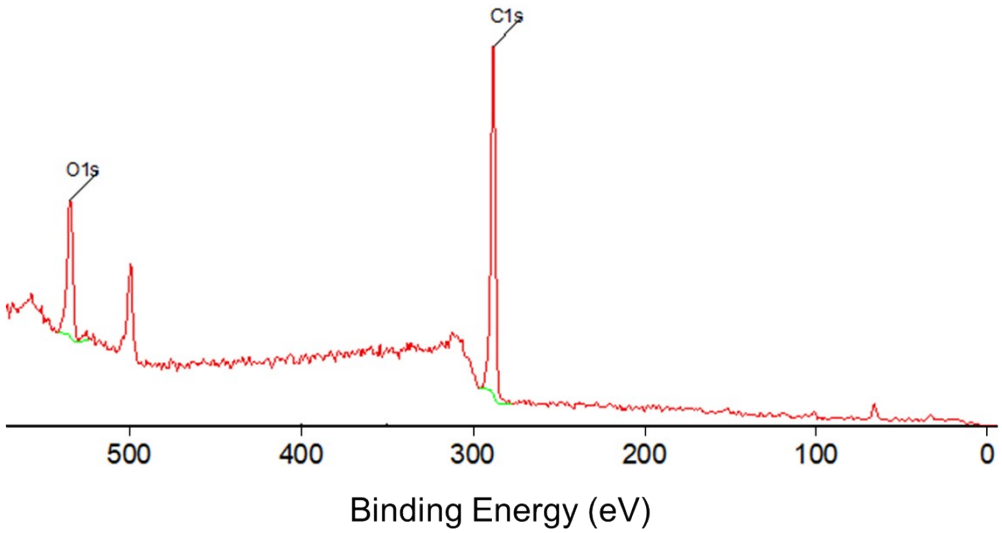

Figure S7. Survey XPS spectra (0-600 eV) for CQDs.

Table S1. The Table compares our work with the Literature indicating the photocatalyst, dye, light source and power, and degradation rate and time. NR stands for not reported.

Photocatalyst	Dye	Light source	Wavelength	Power	Degradation rate	Irradiation time	Reference
Multilayer-GQDs	MB	Led	520 nm and 470 nm	1 $W.mm^{-2}$	93%	60 min	Ref[9]
GQDs and polymer-modified GQDs	MB	Xe lamp	Visible (cutoff λ>400 nm)	300 W	45%	100 min	Ref[10]
GQDs	MB	Sun ligth	Whole spectrum	NR	45%	100 min	Ref[11]
N-CQDs	MB	Xe lamp sun ligth	Visible (cut-off λ>400 nm) / all spectrum	500 W / $(54 \times 10^3 \pm 5000$ lm)	97%	60 min	Ref[12]
N-CQDs	MB	Sun ligth	Whole spectrum	-	95%	180 min	Ref[13]
TiO_2/N-GQDs	MB	UV lamp	UV irradiation	400 W	85%	70 min	Ref[14].
GQDs	Rh G	Sun ligth	Whole spectrum	NR	80%	80 min	Ref[15]
GQDs	MB, MO	CFL and LED	400 and 750 nm	1000 lm	79% / 52%	120 min / 120 min	Ref[16]
GQDs/Polymeric Carbon nitride	Rh B	Xe lamp	Visible (cut-off λ>420 nm)	300 W	100%	80 min	Ref[17]
S,N-GQDs	Crystal violet and Alizarin yellow	Xe lamp	Visible irradiation	400 W	91% / 64%	100 min	Ref[18]
TiO_2/GQDs	Reactive Black 5 (RB5)	Sun ligth	Whole spectrum	NR	100%	30 min	Ref[19]
Crystalline CQDs	MB	Hg lamp	250-750 nm	100 W	95%	5 min	**This study**

References:

(1) Fleischmann, M.; Korinek, K.; Pletcher, D. The Oxidation of Organic Compounds at a Nickel Anode in Alkaline Solution. *J. Electroanal. Chem. Interfacial Electrochem.* **1971**, *31* (1), 39–49. https://doi.org/10.1016/S0022-0728(71)80040-2.

(2) Fleischmann, M.; Korinek, K.; Pletcher, D. The Kinetics and Mechanism of the Oxidation of Amines and Alcohols at Oxide-Covered Nickel, Silver, Copper, and Cobalt Electrodes. *J. Chem. Soc. Perkin Trans. 2* **1972**, No. 10, 1396–1403. https://doi.org/10.1039/P29720001396.

(3) Barbosa, A. F. B.; Oliveira, V. L.; van Drunen, J.; Tremiliosi-Filho, G. Ethanol Electro-Oxidation Reaction Using a Polycrystalline Nickel Electrode in Alkaline Media: Temperature Influence and Reaction Mechanism. *J. Electroanal. Chem.* **2015**, *746*, 31–38. https://doi.org/10.1016/j.jelechem.2015.03.024.

(4) Panagiotopoulou, P.; Antoniadou, M.; Kondarides, D. I.; Lianos, P. Aldol Condensation Products during Photocatalytic Oxidation of Ethanol in a Photoelectrochemical Cell. *Appl. Catal. B Environ.* **2010**, *100* (1), 124–132. https://doi.org/10.1016/j.apcatb.2010.07.021.

(5) Zhao, Y.; Li, X.; Li, Q.; Deng, C. Enhancement of the Photoelectric Performance of Dye-Sensitized Solar Cells by Sol-Gel Modified TiO2 Films. *J. Mater. Sci. Technol.* **2011**, *27* (8), 764–768. https://doi.org/10.1016/S1005-0302(11)60140-0.

(6) Luo, S.; Falconer, J. L. Acetone and Acetaldehyde Oligomerization on TiO2 Surfaces. *J. Catal.* **1999**, *185* (2), 393–407. https://doi.org/10.1006/jcat.1999.2511.

(7) Liu, M.; Xu, Y.; Niu, F.; Gooding, J. J.; Liu, J. Carbon Quantum Dots Directly Generated from Electrochemical Oxidation of Graphite Electrodes in Alkaline Alcohols and the Applications for Specific Ferric Ion Detection and Cell Imaging. *Analyst* **2016**, *141* (9), 2657–2664. https://doi.org/10.1039/C5AN02231B.

(8) Deng, J.; Lu, Q.; Mi, N.; Li, H.; Liu, M.; Xu, M.; Tan, L.; Xie, Q.; Zhang, Y.; Yao, S. Electrochemical Synthesis of Carbon Nanodots Directly from Alcohols. *Chem. – Eur. J.* **2014**, *20* (17), 4993–4999. https://doi.org/10.1002/chem.201304869.

(9) Umrao, S.; Sharma, P.; Bansal, A.; Sinha, R.; Singh, R. K.; Srivastava, A. Multi-Layered Graphene Quantum Dots Derived Photodegradation Mechanism of Methylene Blue. *RSC Adv.* **2015**, *5* (64), 51790–51798. https://doi.org/10.1039/c5ra07310c.

(10) Fan, J.; Li, D.; Wang, X. Effect of Modified Graphene Quantum Dots on Photocatalytic Degradation Property. *Diam. Relat. Mater.* **2016**, *69*, 81–85. https://doi.org/10.1016/j.diamond.2016.07.008.

(11) Kumar, S.; Ojha, A. K.; Ahmed, B.; Kumar, A.; Das, J.; Materny, A. Tunable (Violet to Green) Emission by High-Yield Graphene Quantum Dots and Exploiting Its Unique Properties towards Sun-Light-Driven Photocatalysis and Supercapacitor Electrode Materials. *Mater. Today Commun.* **2017**, *11*, 76–86. https://doi.org/10.1016/j.mtcomm.2017.02.009.

(12) Aghamali, A.; Khosravi, M.; Hamishehkar, H.; Modirshahla, N.; Behnajady, M. A. Synthesis and Characterization of High Efficient Photoluminescent Sunlight Driven Photocatalyst of N-Carbon Quantum Dots. *J. Lumin.* **2018**, *201*, 265–274. https://doi.org/10.1016/j.jlumin.2018.04.061.

(13) Rani, U. A.; Ng, L. Y.; Ng, C. Y.; Mahmoudi, E.; Ng, Y.-S.; Mohammad, A. W. Sustainable Production of Nitrogen-Doped Carbon Quantum Dots for Photocatalytic Degradation of Methylene Blue and Malachite Green. *J. Water Process Eng.* **2021**, *40*, 101816. https://doi.org/10.1016/j.jwpe.2020.101816.

(14) Safardoust-Hojaghan, H.; Salavati-Niasari, M. Degradation of Methylene Blue as a Pollutant with N-Doped Graphene Quantum Dot/Titanium Dioxide Nanocomposite. *J. Clean. Prod.* **2017**, *148*, 31–36. https://doi.org/10.1016/j.jclepro.2017.01.169.
(15) Ahmed, B.; Kumar, S.; Ojha, A. K.; Hirsch, F.; Riese, S.; Fischer, I. Facile Synthesis and Photophysics of Graphene Quantum Dots. *J. Photochem. Photobiol. Chem.* **2018**, *364*, 671–678. https://doi.org/10.1016/j.jphotochem.2018.07.006.
(16) Ibarbia, A.; Grande, H. J.; Ruiz, V. On the Factors behind the Photocatalytic Activity of Graphene Quantum Dots for Organic Dye Degradation. *Part. Part. Syst. Charact.* **2020**, *37* (5), 2000061. https://doi.org/10.1002/ppsc.202000061.
(17) Cheng, L.; Dong, X. Carbonaceous 0D/2D Composite Photocatalyst for Degradation of Organic Dyes. *Diam. Relat. Mater.* **2020**, *109*, 108096. https://doi.org/10.1016/j.diamond.2020.108096.
(18) Selvakumar, T.; Rajaram, M.; Natarajan, A.; Harikrishnan, L.; Alwar, K.; Rajaram, A. Highly Efficient Sulfur and Nitrogen Codoped Graphene Quantum Dots as a Metal-Free Green Photocatalyst for Photocatalysis and Fluorescent Ink Applications. *ACS Omega* **2022**, *7* (15), 12825–12834. https://doi.org/10.1021/acsomega.2c00092.
(19) Niazi, Z.; Goharshadi, E. K.; Mashreghi, M.; Jorabchi, M. N. Highly Efficient Solar Photocatalytic Degradation of a Textile Dye by TiO_2/Graphene Quantum Dots Nanocomposite. *Photochem Photobiol Sci* **2021**, *20* (1), 87–99. https://doi.org/10.1007/s43630-020-00005-7.